Influences of semiconductor laser on fibre-optic distributed disturbance sensor based on Mach–Zehnder interferometer

Liang Sheng(梁 生)[a†], Zhang Chun-Xi(张春熹)[a], Lin Bo(蔺 博)[b], Lin Wen-Tai(林文台)[a], Li Qin(李 勤)[a], Zhong Xiang(钟 翔)[a], and Li Li-Jing(李立京)[a]

[a] *School of Instrument Science and Opto-Electronics Engineering, Beihang University, Beijing* 100191, *China*
[b] *Photonics Research Centre, School of Electrical and Electronic Engineering, Nanyang Technological University,* 50 *Nanyang Avenue,* 639798, *Singapore*

(Received 31 May 2010; revised manuscript received 10 June 2010)

This paper investigates the influences of a semiconductor laser with narrow linewidth on a fibre-optic distributed disturbance sensor based on Mach–Zehnder interferometer. It establishes an effective numerical model to describe the noises and linewidth of a semiconductor laser, taking into account their correlations. Simulation shows that frequency noise has great influences on location errors and their relationship is numerically investigated. Accordingly, there is need to determine the linewidth of the laser less than a threshold and obtain the least location errors. Furthermore, experiments are performed by a sensor prototype using three semiconductor lasers with different linewidths, respectively, with polarization maintaining optical fibres and couplers to eliminate the polarization induced noises and fading. The agreement of simulation with experimental results means that the proposed numerical model can make a comprehensive description of the noise behaviour of a semiconductor laser. The conclusion is useful for choosing a laser source for fibre-optic distributed disturbance sensor to achieve optimized location accuracy. What is more, the proposed numerical model can be widely used for analysing influences of semiconductor lasers on other sensing, communication and optical signal processing systems.

Keywords: fibre-optic distributed sensor, semiconductor laser, narrow linewidth laser, fibre-optic interferometric sensor

PACC: 4281P, 4285F

1. Introduction

Fibre-optic distributed disturbance sensor (FDDS) has attracted a lot of interests for different applications in intrusion detection,[1−17] pipeline monitoring[1−17] and acoustic emission sensing.[18] Interferometric FDDS is greatly utilized in these applications due to its high sensitivity and capability of locating the disturbance in comparison with the other sensing approaches.[1−19] The configurations of the interferometric FDDSs can be classified into the following categories: Sagnac interferometer (SI) and Mach–Zehnder interferometer (MZI),[1,2] SI and Michelson interferometer (MI),[3−6] dual SIs,[7−10] single SI,[11−13] SI with dual-wavelength[14,15] or working in dual-mode[16] and differentiating ring.[17]

When SI merges with MZI or MI to form an FDDS, one problem is that a low coherent light source is required for SI, while a highly coherent stable laser source is needed for the MZI or MI. In the single SI configuration, the locating arithmetic is complicated and the sensitivity depends on the location of disturbance. For dual SIs and single SI with dual-wavelength or working in dual-mode, the high cost for double light sources and photo-detectors, modulators with different frequency for dual-mode system and wavelength division multiplexing (WDM) for dual-wavelength system prevent the further practical applications. In contrast, owing to its simple configuration and straightforward location arithmetic, MZI is considered as a low cost and effective approach to produce an FDDS.[18,19]

For MZI-based FDDS, location accuracy is the most important characteristic for practical applications. Also, the type of the used light source is very crucial for interferometric sensors. A semiconductor laser (SCL) is often employed for high coherence applications due to its unique advantages such as low

†Corresponding author. E-mail: liangsheng2008@yahoo.com.cn
© 2010 Chinese Physical Society and IOP Publishing Ltd

cost, convenient use and compactness.[20−22] However, noises from an SCL limit the resolution and accuracy of an interferometric sensor. Therefore, it is necessary to investigate the influences of an SCL on the location accuracy of an MZI-based FDDS. So far, several works have been presented to establish the internal numerical models for SCLs to optimize the design and improve the performances.[23,24] Some works have also been reported to analyse the influences of SCLs on fibre-optic communication systems[25] and coherent optical frequency domain reflectometry.[26] However, no particular work provided detailed analysis and explanation of the influences of SCLs on interferometric fibre-optic distributed sensors, which is focused in this paper.

2. Principle of MZI-based FDDS

The schematic diagram of the proposed MZI-based FDDS is illustrated in Fig. 1. The light from a laser source launches into a 3-dB optical coupler (coupler 1) and splits into two paths: one operates in the clockwise MZI and the other operates in the counter-clockwise MZI. Once a disturbance exists on the fibre, a change in phase $\Delta\varphi$ between the two arms of MZI will occur. The signals received by photo-detectors (PDs) 1 and 2 from the clockwise and counter-clockwise MZIs, respectively, can be expressed as

$$I_1(t) = I_1\{1 + K_1 \cos[\Delta\varphi(t - t_1) + \varphi_0]\}, \quad (1)$$

$$I_2(t) = I_2\{1 + K_2 \cos[\Delta\varphi(t - t_2 - t_3) + \varphi_0]\}, \quad (2)$$

where t_1, t_2, t_3 are the propagating time through the fibres L_1, L_2, L_3, respectively. Here the distances from laser source to coupler 1 and from PD 2 to coupler 2 are neglected. The I_1 and I_2 are determined by the input intensity of the interferometers and the total loss of the fibre. The K_1 and K_2 are the visibilities of the dual MZIs and approximately equal 1 for simplicity by neglecting the polarization induced fading in the single mode fibre. The φ_0 is the initial phase caused by the difference between the two arms of MZI. There is a time delay difference Δt between $I_1(t)$ and $I_2(t)$: $\Delta t = t_2 + t_3 - t_1$. Hence the location of disturbance can be obtained from the time delay difference Δt,

$$L_1 = \frac{1}{2}(L - c\Delta t/n), \quad (3)$$

where $L = L_1 + L_2 + L_3$. Calculating the cross correlation function of $I_1(t)$ and $I_2(t)$, and finding the time value according to the extremum of the cross correlation function, we can obtain Δt.

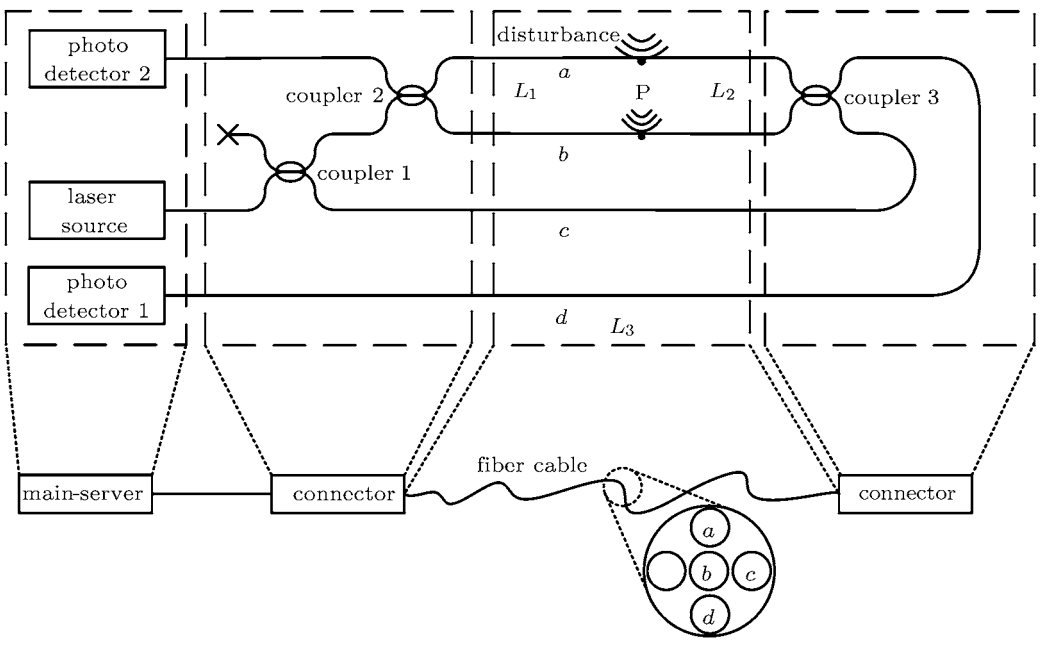


Fig. 1. Schematic illustration of the MZI-based FDDS.

3. Noises of semiconductor laser

Generally, SCL is considered as a relatively low-noise light source, however, there are still some noises which prevent further applications with requirement of improved performances. In general, noises of an SCL can be mainly classified into four types: dynamical, cavity, thermal and acoustic noises.[23−44] Dynamical noises are associated with direct perturbations to the dynamical variables of the laser, namely the pump, gain medium and laser field, and induced by the spontaneous emission and variation of the real refractive index with carrier density fluctuations. Cavity noise (or kinematic noise) is associated with perturbations to the resonant structure including passive medium. Thermal and acoustic noises are external noises such as self-heating associated with nonradiative transitions. In this paper, the dynamical noises of SCL are investigated as the main internal noises, which make great influences on the interferometric sensor.

Due to its dynamical noises, SCL presents frequency noise (FN), phase noise (PN) and relative intensity noise (RIN).

Considering the noises, we can express the instantaneous frequency of laser as

$$\upsilon_0(t) = \upsilon_0 + \Delta\upsilon_0(t), \tag{4}$$

where υ_0 is the work frequency and the fluctuation of frequency $\Delta\upsilon_0(t)$ is defined as FN, which consists of white, $1/f$ (or flicker) and other components. The formula expression of FN can be written as

$$\begin{aligned}\Delta\upsilon_0(t) &= FN(t) = FN_{\rm white}(t) + FN_{1/f}(t) \\ &\quad + FN_{\rm other}(t),\end{aligned} \tag{5}$$

where $FN_{\rm white}(t)$ is the white FN, $FN_{1/f}(t)$ is the $1/f$ FN and $FN_{\rm other}(t)$ is the FN induced by other factors, such as mode hopping,[39−41] which is neglected in our analysis for simplicity because mode hopping has been effectively suppressed in commercial SCLs.

The power spectral density of FN can be expressed as[28−39]

$$S_{\rm FN}(f) = C/P + K/f + S_{\rm other}(f), \tag{6}$$

where C/P denotes the white component and K/f is the $1/f$ component, $C = 1.5 \times 10^4$ Hz/W and $K = 5.8 \times 10^{11}$ Hz^2.[28] At low frequencies (0 to 100 kHz), FN is dominated by $1/f$ noise, whose origin can be considered as arising from fluctuations of the charge carriers or the pumping. For frequencies above 100 kHz, white noise induced by spontaneous emission tends to play a main role, though it scales inversely with laser power. In contrast, the magnitude of $1/f$ noise is essentially independent of the laser power. Therefore, $1/f$ noise becomes more significant than the spontaneous emission noise in the limit of high output powers.

Accordingly, the PN is induced through an unbalanced MZI and can be derived by

$$\begin{aligned}PN(t) &= 2\pi n_{\rm eff} \cdot \Delta L \cdot \Delta\upsilon_0(t)/c \\ &= 2\pi n_{\rm eff} \cdot \Delta L \cdot FN(t)/c,\end{aligned} \tag{7}$$

where $n_{\rm eff}$ is the effective refractive index of fibre core and ΔL is the length difference between the two arms of MZI.

Linewidth of SCL is correlative to the FN, which is assumed to result from the phase fluctuation of the laser field induced by two independent processes, one of which is the phase change caused directly by each spontaneous emission event and the other is the change of the cavity resonance frequency due to the refractive index change caused by the carrier density fluctuation.[28−39]

The linewidth of SCL is determined by FN and can be expressed as

$$\begin{aligned}\Delta\upsilon(t) &= \Delta\upsilon_{\rm w}(t) + \Delta\upsilon_{\rm r}(t) + \Delta\upsilon_{\rm other}(t) \\ &= \pi \cdot S_{\rm w-FN}(t) + r \cdot S_{1/f-{\rm FN}}(t) \\ &\quad + \Delta\upsilon_{\rm other}(t),\end{aligned} \tag{8}$$

where $\Delta\upsilon(t)$ is the linewidth, $\Delta\upsilon_{\rm w}(t)$ is the linewidth induced by the white FN, $\Delta\upsilon_{\rm r}(t)$ is the residual linewidth due to the $1/f$ FN and r is the coefficient of residual linewidth. The $\Delta\upsilon_{\rm other}(t)$ is the linewidth induced by other factors, such as modulation of current which is neglected here. It is worth while noting that the linewidth broadening induced by side mode is neglected due to the high side mode suppression ratio (40 dB). The resulting line shape of SCL is the convolution of the Lorentzian shape due to the white FN and the approximate Gaussian shape arising from $1/f$ FN. The convolution of a Lorentzian and a Gaussian shape presents a Voigt profile.[43,44] However, available approximation can be achieved by a Gaussian line shape especially for the case of narrow linewidth.

The power fluctuation of SCL is defined by the intensity noise and can be calculated by

$$I_0(t) = I_0 + \Delta I_0(t) = I_0(1 + \sqrt{RIN(t)} \cdot B), \tag{9}$$

where $I_0(t)$ is the instantaneous power, I_0 is the work power, $\Delta I_0(t)$ is the fluctuation of power, $RIN(t)$ is the relative intensity noise (RIN) of unit bandwidth, and B is the detection bandwidth.

4. Simulation and results

Assuming that the spectrum of an SCL is Gaussian profile, we can derive the coherent function as

$$\gamma_{\rm G}(\tau,t)=\exp[-\tau^2(t)/4\tau_{\rm c}^2(t)], \tag{10}$$

where the coherent time is given by

$$\tau_{\rm c}(t)=1/4\pi\Delta f(t), \tag{11}$$

where $\Delta f(t)=\Delta\lambda(t)/\lambda_0^2(t)$, $\Delta\lambda(t)=\Delta\upsilon(t)/[\upsilon_0^2(t)\cdot c]$ and $\lambda_0(t)=c/\upsilon_0(t)$ is the wavelength of laser.

The intensity of interference light can be expressed as

$$I(t)=\frac{I_{\rm in}(t)}{2}\{1+\gamma_{\rm G}[\tau(t),t]\cdot\cos[2\pi\upsilon_0(t)\cdot\tau(t)]\}, \tag{12}$$

where $\tau(t)=\tau_0+dis(t)$ is the time delay difference between the two interference beams, $\tau_0=n_{\rm eff}\cdot\Delta L/c$ is the time delay difference related to the length difference between the two arms of MZI, $dis(t)$ is the time delay modulation caused by the disturbance.

The optical signals detected by the PDs 1 and 2 from clockwise and counter-clockwise MZIs can be expressed as

$$I_1(t)=\frac{I_{\rm in1}(t+\Delta t)}{2}\{1+\gamma_{\rm G1}[\tau(t+\Delta t),t+\Delta t]\cdot\cos[2\pi\upsilon_{01}(t+\Delta t)\cdot\tau(t+\Delta t)]\}, \tag{13}$$

$$I_2(t)=\frac{I_{\rm in2}(t)}{2}\{1+\gamma_{\rm G2}[\tau(t),t]\cdot\cos[2\pi\upsilon_{02}(t)\cdot\tau(t)]\}, \tag{14}$$

where Δt is the time delay between the two signals from the two MZIs.

Taking into account the laser noises, we find that the two beams arriving at a particular disturbance point P (see Fig. 1) undergo different time durations, so that the instantaneous frequency and power of the two light beams are different. Frequency of the clockwise and counter-clockwise light beams can be expressed respectively as

$$\begin{aligned}\upsilon_{01}(t) &= \upsilon_0+\Delta\upsilon_0(t-\Delta t)=\upsilon_0+FN(t-\Delta t)\\ &= \upsilon_0+FN_{\rm white}(t-\Delta t)+FN_{1/f}(t-\Delta t)+FN_{\rm other}(t-\Delta t),\end{aligned} \tag{15}$$

$$\upsilon_{02}(t) = \upsilon_0+\Delta\upsilon_0(t)=\upsilon_0+FN(t)=\upsilon_0+FN_{\rm white}(t)+FN_{1/f}(t)+FN_{\rm other}(t). \tag{16}$$

Accordingly, the linewidth is given by

$$\Delta\upsilon_1(t)=\Delta\upsilon_{\rm white}(t-\Delta t)+\Delta\upsilon_{\rm residual}(t-\Delta t)=\pi\cdot FN_{\rm white}(t-\Delta t)+r\cdot FN_{1/f}(t-\Delta t), \tag{17}$$

$$\Delta\upsilon_2(t)=\Delta\upsilon_{\rm white}(t)+\Delta\upsilon_{\rm residual}(t)=\pi\cdot FN_{\rm white}(t)+r\cdot FN_{1/f}(t). \tag{18}$$

The power can be derived by

$$I_{\rm in1}(t)=[I_0+\Delta I_{\rm in}(t-\Delta t)]/2=\{I_0[1+\sqrt{RIN(t-\Delta t)}\cdot B]\}/2, \tag{19}$$

$$I_{\rm in2}(t)=[I_0+\Delta I_{\rm in}(t)]/2=\{I_0[1+\sqrt{RIN(t)}\cdot B]\}/2. \tag{20}$$

To simplify the analysis, the noise from PD is neglected and the used SCL is assumed to be temperature stabilized. The thermal noise is also neglected. The simulation is carried out by using the MATLAB and the initialized parameters of both SCL and FDDS are summarized in Table 1.

In an MZI-based FDDS, the most significant characteristic is the location accuracy, which is usually decided by calculating the maximal location error with several measurements of disturbances at a particular location. The noise influences of the SCL on the maximal location error are analysed in simulation.

As a particular example, figures 2, 3 and 4 show FN of SCL, power spectrum density of FN and RIN of SCL respectively. We use the parameters shown in Table 1 in calculations, especially $\Delta L=50$ m, $\Delta\nu=50$ kHz, $L_1=30$ km, $RIN=-155$ dB and the location error is 0 m in this case.

Table 1. Summary of initialized SCL and FDDS parameters for simulation.

symbol	description	value	unit
	parameters of SCL		
$A_{\rm FN}$	amplitude of FN	10∼10^7	kHz
RIN	amplitude of RIN	–155∼–125	dB
r	coefficient for residual linewidth	~ 1	–
$\Delta\nu$	linewidth of SCL	1∼2×10^3	kHz
λ_0	wavelength of SCL	1550	nm
	parameters of FDDS		
$f_{\rm s}$	sampled frequency	10	MHz
L	monitored length	50	km
ΔL	difference between two arms of MZI	0∼50	m
L_1	location of disturbance	0∼ L	m

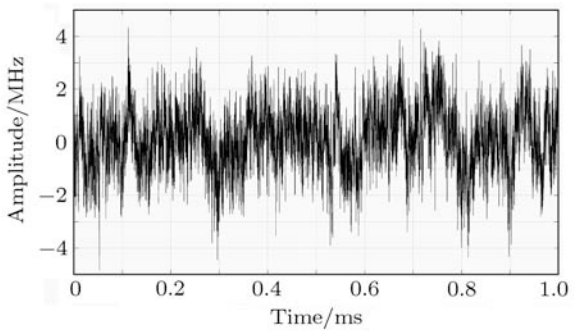


Fig. 2. The FN of SCL.

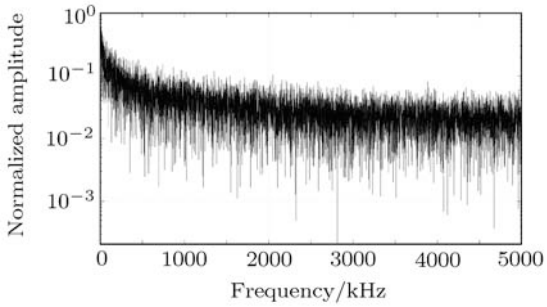


Fig. 3. Power spectrum density of FN.

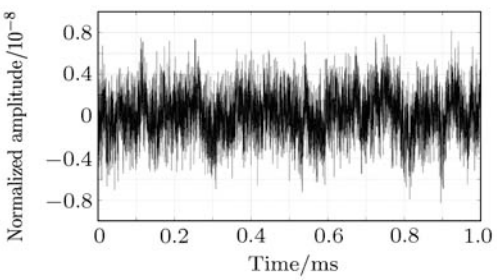


Fig. 4. The RIN of SCL.

The variations of maximal location errors as a function of FN amplitude and laser linewidth at different disturbance locations (L_1) are shown in Figs. 5 and 6, respectively. We implement ten times simulations for each particular disturbance location with the same parameters except using different noise sequences. The maximal location errors are decided from the ten simulation results.

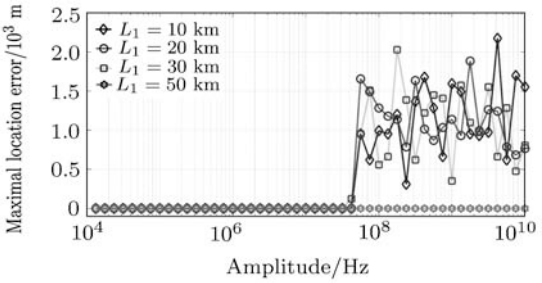


Fig. 5. Relationship between maximal location error and amplitude of FN with different locations (L_1).

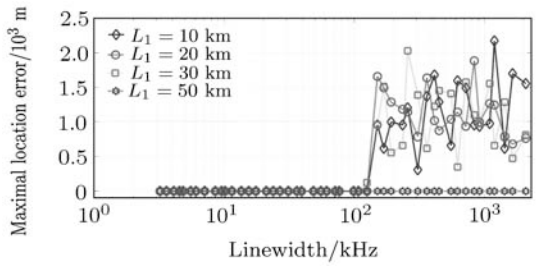


Fig. 6. Relationship between maximal location error and linewidth with different locations (L_1).

It can be seen from Fig. 6, the distribution of maximal location errors exhibits a "high pass"-like curve except for the case of $L_1 = 50$ km, which illustrates that a threshold of laser linewidth exists in order to achieve zero location errors. In addition, the laser linewidth threshold is independent of the disturbance location when $L_1 \neq 50$ km. In our simulation, a typical threshold for SCL linewidth is about 100 kHz.

In fact, the coherent length of an SCL with a 100-kHz linewidth is about 2.5 km, which is much larger

than the length difference between two arms of MZI (10 m for this case). It is also known that, the location accuracy is greatly affected by the FN of an SCL if the linewidth exceeds the threshold. The reason is that for the distributed interferometric sensor, the instantaneous frequency υ_0 of the light wave modulated by a disturbance at position P is stochastic, and thus the initialized phase (φ_0) and modulated signal phase (φ_s) between the clockwise and counter-clockwise MZIs are different. As a result, the correlation between two signals from MZIs is destroyed. Hence, the location error occurs. The fluctuation of the location errors is led by the statistical characteristic of noises, when FN and linewidth exceed threshold.

For the special case with $L_1 = 50$ km, the time durations of light wave transmitting from the SCL to position P through clockwise and counter-clockwise are same. Hence, there is no influence of FN on the location error.

To understand the impact of the length difference between two arms of MZIs (ΔL) on the laser linewidth threshold, the maximal location error and FN (linewidth) with different ΔL are analysed and shown in Figs. 7 and 8, respectively, in both the cases, L_1 is fixed at 30 km. It is clear that there is no distinct influence on the SCL linewidth threshold when

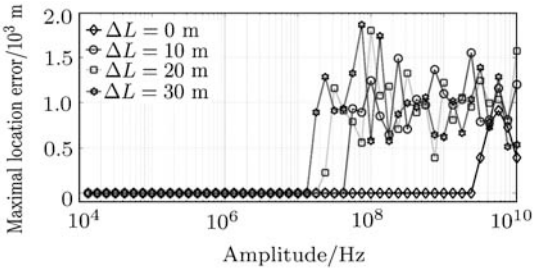


Fig. 7. Relationship between maximal location error and amplitude of FN with different differences between two arms of MZI (ΔL).

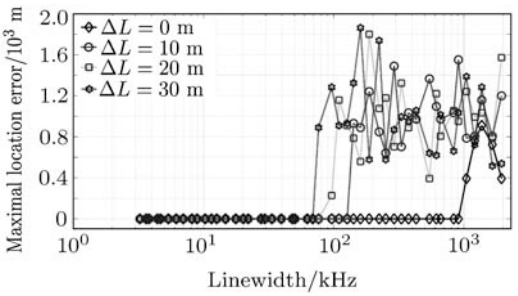


Fig. 8. Relationship between maximal location error and linewidth with different differences between two arms of MZI (ΔL).

$\Delta L \neq 0$. While ΔL decreases to 0, the threshold of FN and linewidth increases. Because in the case of $\Delta L = 0$, the influence of difference of initialized phases (ϕ_0) between clockwise and counter-clockwise MZIs is eliminated. It should be noted that, $\Delta L = 0$ is an ideal case, and for practical applications, ΔL cannot equal 0 strictly.

Figure 9 shows the effect of laser RIN to maximal location error at two different SCL linewidths (one linewidth is above the threshold and the other is below). It can be found that there is no distinct influence of the RIN on the location error when RIN is lower than −60 dB, which is generally realized by current commercial SCL products.

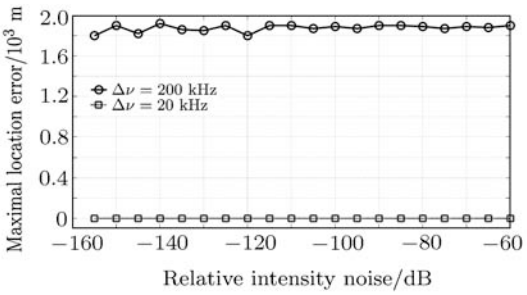


Fig. 9. Relationship between maximal location error and RIN with different linewidths.

From above-mentioned simulation results, we believe that FN of an SCL is the most important factor leading influence on the location error of an MZI-based FDDS. It is important to choose an SCL with suitable linewidth. Not only SCL's coherent length but also the threshold of linewidth should be taken into consideration. Furthermore, when laser linewidth can be chosen in a range of values less than the threshold, taking into account other cases such as suppression of scattering noises and so on is necessary and feasible. Considering the combined effect, we find that there may be an optimum linewidth which can achieve the optimum location accuracy.

5. Experimental results and discussion

To validate the simulation results, we implemented an experiment by an MZI-based FDDS prototype using three SCLs with different linewidths, respectively. The SCLs employed in our experiments are shown in Table 2. The polarization maintaining optical fibres and couplers were utilized to eliminate

the influences of polarization induced noises and fading. In the experiment, some parameters in Table 1 are changed due to our setup limitation. The monitored length is 1 km, $\Delta L \approx 5$ m, $L_1 = 0$ km and the sampling frequency is 2 MHz. Simulation based on these parameters is also carried out.

Table 2. Summary of employed SCLs in experiments.

NO.	$\Delta\nu$	model
I	5 kHz	denslight: DL-BF12
II	25 kHz	emcore: 1792 ECCW
III	1 MHz	emcore: 1772

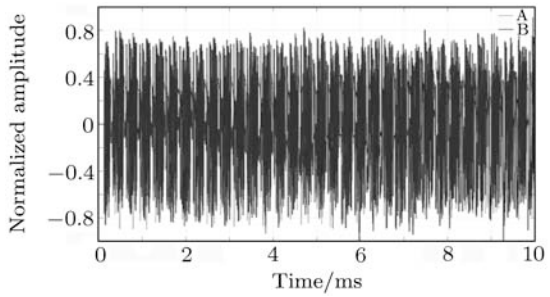


Fig. 10. Normalized signals from clockwise (A) and counter-clockwise (B) MZI ($\Delta\nu = 25$ kHz).

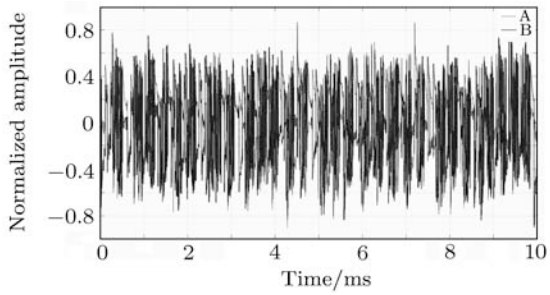


Fig. 11. Normalized signals from clockwise (A) and counter-clockwise (B) MZI ($\Delta\nu = 1$ MHz).

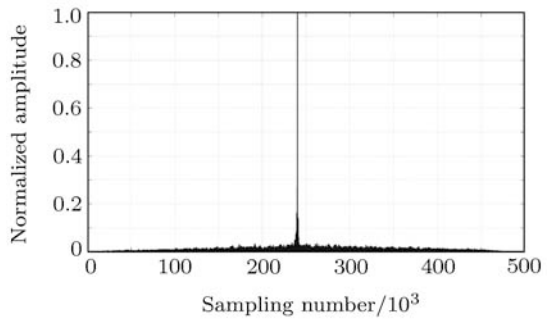


Fig. 12. Normalized cross correlation function ($\Delta\nu = 25$ kHz).

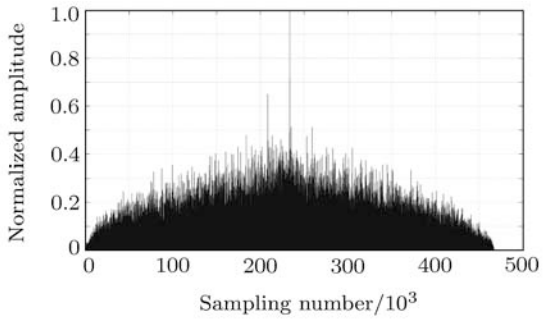


Fig. 13. Normalized cross correlation function ($\Delta\nu = 1$ MHz).

In the cases of $\Delta\nu = 25$ kHz and 1 MHz, signals from PDs 1 and 2 and cross correlation functions are illustrated in Figs. 10–13, respectively. Furthermore, simulated and experimental results of relationship between maximal location error and linewidth are shown in Fig. 14. The maximal location errors are 0 km (SCLs I and II) and 4 km (SCL III), respectively. The numerically simulated and experimentally measured results are in good agreement with each other.

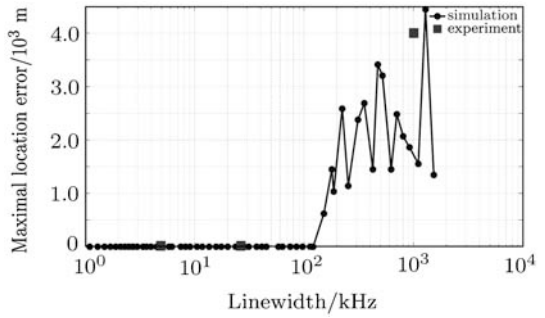


Fig. 14. Experimental results of maximal location errors using different lasers. Linewidth: 5 kHz (SCL I), 25 kHz (SCL II) and 1 MHz (SCL III).

6. Conclusion

The influences of fibre-optic distributed disturbance sensor based on a Mach–Zehnder interferometer have been demonstrated theoretically and experimentally. A numerical model for semiconductor laser is established to describe the frequency noise, relative intensity noise and linewidth taking into account their correlation. Simulation results show that the location error is determined by the frequency noise, that is, laser induces zero location errors when the frequency noise (laser linewidth) is less than a threshold (a typical value for linewidth is 100 kHz in our simulation), while location errors are caused when exceeding the threshold. Experiments are implemented

by using a sensor prototype employing three semiconductor lasers with different linewidths, respectively, with polarization maintaining optical fibres and couplers to eliminate the influences of polarization. The satisfactory agreement of the simulation with the experimental results proves that the proposed numerical model can make a comprehensive description of the noise behaviour of narrow linewidth semiconductor laser. The conclusion is useful for choosing laser source for sensor. This numerical model can be widely used for analysing influences of laser on other sensing, communication and optical signal processing systems.

Acknowledgment

The author S. Liang would like to acknowledge the support by the Innovation Foundation of Beihang University for Ph.D Graduates.

References

[1] Chtcherbakov A A, Swart P L, Spammer S J and Lacquet B M 1998 *The Fourth Pacific Northwest Fibre Optic Sensor Workshop* (Troutdale, USA May 1998) p. 60
[2] Chtcherbakov A A, Swart P L and Spammer S J 1998 *Appl. Opt.* **37** 3432
[3] Spammer S J, Swart P L and Chtcherbakov A A 1997 *J. Lightwave Technol.* **15** 972
[4] Kondrat M, Szustakowski M, Pałka N, Ciurapiński W and Życzkowski M 2007 *Opto-Electron. Rev.* **15** 127
[5] Chtcherbakov A A and Swart P L 1998 *J. Lightwave Technol.* **16** 1404
[6] Udd E 1996 *Smart Structures and Materials 1996: Smart Systems for Bridges, Structures and Highways* (San Diego, USA Feb. 1996) p. 210
[7] Rønnekleiv E 1997 *Appl. Opt.* **36** 2076
[8] McAulay A D and Wang J 2004 *Proc. SPIE* **5435** p. 114
[9] Fang X J 1996 *J. Lightwave Technol.* **14** 2250
[10] Szustakowski M, Jaroszewicz L R and Kiezun A 1994 *Interferometry '94: Interferometric Fiber Sensing* (Warsaw, Poland May 1994) p. 84
[11] Hoffman P R and Kuzyk M G 2004 *J. Lightwave Technol.* **22** 494
[12] Wu D F, Zhang T Z and Jia B 2008 *Microwave Opt. Technol. Lett.* **50** 1608
[13] Lin W W 2004 *Opt. Eng.* **43** 278
[14] Russell S J, Brady K R C and Dakin J P 2001 *J. Lightwave Technol.* **19** 205
[15] Spammer S J, Swart P L and Chtcherbakov A A 1998 *Microwave Opt. Technol. Lett.* **17** 170
[16] Fang X J 1996 *Opt. Lett.* **21** 444
[17] Spammer S J, Swart P L and Booysen A 1996 *Appl. Opt.* **34** 3200
[18] Liang S, Zhang C X, Lin W T, Li L J, Li C, Feng X J and Lin B 2009 *Opt. Lett.* **34** 1858
[19] Sun Q Z, Liu D M and Wang J 2007 *Acta Phys. Sin.* **56** 5903 (in Chinese)
[20] Bartolo1 R E, Tveten A and Kirkendal C K 2009 *20th International Conference on Optical Fibre Sensors* (Edinburgh, UK Oct. 2009) p. 750370
[21] Alalusi M, Brasil P, Lee S, Mols P, Stolpner L, Mehnert A and Li S 2009 *Proc. SPIE* **7316** 73160X
[22] Bartolo R E and Kirkendall C K 2006 *Proc. SPIE* **6133** p. 61330I
[23] Daniel L, Martin V L and Carlos F 2007 *International Conference on Numerical Simulation of Semiconductor Optoelectronic Devices — NUSOD'07* (Newark, DE Sep. 2007) p. 73
[24] Fatadin I, Ives D and Wicks M 2006 *IEEE J. Quantum Electron.* **42** 934
[25] Sato T 2004 *J. Lightwave Technol.* **22** 1782
[26] Boukari O, Hassine L and Bouchriha H 2010 *Opt. Commun.* **283** 1880
[27] Charles H H 1982 *IEEE J. Quantum Electron.* **QE-18** 259
[28] Kikuchi K 1989 *IEEE J. Quantum Electron.* **25** 684
[29] Ishida O 1990 *IEEE Photon. Technol. Lett.* **2** 784
[30] Cliche J F, Allard M and Têtu M 2006 *Proc. SPIE* **6216** p. 62160C
[31] Charles C H 1986 *J. Lightwave Technol.* **LT-4** 298
[32] Turner L D, Weber K P, Hawthorn C J and Scholten R E 2002 *Opt. Commun.* **201** 391
[33] Ferreira M F S, Rocha J R F and Pinto J L 1992 *IEEE J. Quantum Electron.* **28** 833
[34] Agrawal G P 1989 *IEEE Photon. Technol. Lett.* **1** 212
[35] Guo C Z and Huang Y Z 1989 *Acta Phys. Sin.* **38** 699 (in Chinese)
[36] Liu C, Ge J H and Chen J 2006 *Acta Phys. Sin.* **55** 5211 (in Chinese)
[37] Tian X T, Li Y M, Liu Q and Zhang K S 2009 *Chin. Phys.* B **18** 2324
[38] Zhang Z G, Guo S X, Gao F L, Yu S Y and Li X Y 2009 *Acta Phys. Sin.* **58** 2772 (in Chinese)
[39] Chen D Y and Wang Z L 2009 *Acta Phys. Sin.* B **58** 1403 (in Chinese)
[40] Bager L 1990 *IEEE Photon. Technol. Lett.* **2** 899
[41] Ohtsij M, Teramachi Y, Otsuka Y and Osaki A 1986 *IEEE J. Quantum Electron.* **QE-22** 535
[42] Heumier T A and Carlsten J L 1993 *IEEE J. Quantum Electron.* **29** 2756
[43] Stephan G M, Tam T T, Blin S, Besnard P and Têtu M 2005 *Phys. Rev.* A **71** 043809
[44] Fermigier B and Têtu M 1998 *Proc. SPIE* **3415** p. 164